Recurrent genomic alterations characterize medulloblastoma arising from DNA double-strand break repair deficiency

Pierre-Olivier Frappart[a,1], Youngsoo Lee[a,1], Helen R. Russell[a], Nader Chalhoub[b], Yong-Dong Wang[c], Kenji E. Orii[a,d], Jingfeng Zhao[a], Naomi Kondo[d], Suzanne J. Baker[b], and Peter J. McKinnon[a,2]

Departments of [a]Genetics and Tumor Cell Biology and [b]Developmental Neurobiology, and [c]Hartwell Center for Biotechnology, St. Jude Children's Research Hospital, Memphis, TN 38105; and [d]Department of Pediatrics, Gifu University Graduate School of Medicine, Gifu 501-1194, Japan

Edited by James E. Cleaver, University of California, San Francisco, CA, and approved December 9, 2008 (received for review July 16, 2008)

Inactivation of homologous recombination (HR) or nonhomologous end-joining (NHEJ) predisposes to a spectrum of tumor types. Here, we inactivated DNA double-strand break repair (DSBR) proteins, DNA Ligase IV (Lig4), Xrcc2, and Brca2, or combined Lig4/Xrcc2 during neural development using Nestin-cre. In all cases, inactivation of these repair factors, together with p53 loss, led to rapid medulloblastoma formation. Genomic analysis of these tumors showed recurring chromosome 13 alterations via chromosomal loss or translocations involving regions containing *Ptch1*. Sequence analysis of the remaining *Ptch1* allele showed a variety of inactivating mutations in all tumors analyzed, highlighting the critical tumor suppressor function of this hedgehog-signaling regulator. We also observed genomic amplification or up-regulation of either *N-Myc* or *cyclin D2* in all medulloblastomas. Additionally, chromosome 19, which contains Pten, was also selectively deleted in medulloblastoma arising after disruption of HR. Thus, our data highlight the preeminence of Ptch1 as a tumor suppressor in cerebellar granule cells and reveal other genomic events central to the genesis of medulloblastoma.

DNA strand breaks | patched1 | sonic hedgehog | cerebellum

Repair of DNA double-strand breaks (DSBs) can occur via nonhomologous end joining (NHEJ) or homologous recombination (HR). A distinguishing feature between these pathways is the requirement of HR for a sister chromatid present in the S/G_2 phase of replicating cells to provide an error-free template for DNA repair (1, 2). Multiple factors coordinate HR, and among these, Xrcc2 and Brca2 are critical (1). In contrast to HR, NHEJ is an error-prone repair mechanism that enzymatically modifies the 2 ends of a DNA break so that they are compatible for direct ligation (2, 3). Of the factors important for NHEJ, DNA ligase IV (Lig4), which functions together with Xrcc4, is required for ligation of DNA ends. During development of the central nervous system (CNS), HR is required to prevent genomic instability in proliferative progenitor cells, whereas NHEJ is critical in postmitotic neurons (4). Inactivation of either pathway can perturb development of the nervous system, leading to defective neurogenesis, microcephaly, or brain tumors (5).

Medulloblastoma is the most common malignant pediatric brain tumor, and it often arises from the granule neuron progenitors (GNPs) in the external germinal layer of the developing cerebellum (6, 7). Many medulloblastoma models have a gene expression profile very similar to GNPs (8–12). However, medulloblastoma is a disease comprising multiple subtypes that presumably arise either from disparate progenitor cells or as a result of mutations in different signaling pathways (6, 7). Several rare human syndromes, such as Turcot (*APC* germ-line mutation), Gorlin (*PTCH1* germ-line mutation), Fanconi anemia complementation group D1 (*BRCA2* germ-line mutation), or Nijmegen Breakage (*NBS1* hypomorphic mutation), predispose to medulloblastoma (7, 13–15). Additionally, mutations of multiple genes involved in the sonic hedgehog (SHH) pathway, including *PTCH1*, *SUFU*, *SMOH*, or the Wingless (*WNT*) pathway, such as *AXIN1* or *β-CATENIN*, have also been found in sporadic human medulloblastomas, highlighting the importance of these pathways for preventing cancer (16). Although mutations of the p53 pathway occur in sporadic medulloblastomas (<20%), inactivation of the p53 pathway may be prevalent (9, 14, 17, 18).

Consistent with the above, 5–15% of *Ptch1* heterozygote mice develop medulloblastoma by 8 months of age (depending on the genetic background), an event that is associated with inactivation of the remaining *Ptch1* allele (19–21). Loss of *p53* or *Ptch2* significantly increases the incidence of medulloblastoma in $Ptch1^{+/-}$ mice (20, 22). Although p53-null mice are not predisposed to develop medulloblastoma (23, 24), *p53* loss is a prerequisite in many models of medulloblastoma (10–12, 22, 25–27). Inactivation of proteins involved in NHEJ, such as Lig4, Xrcc4, and Ku80, or HR, such as Xrcc2 or Brca2, also leads to medulloblastoma formation in a p53-deficient background (4, 26–29). Radiation-induced medulloblastoma acceleration in $Ptch1^{+/-}$ mice also suggests that DNA damage in the developing cerebellum strongly predisposes to tumorigenesis (30).

To further examine the genesis of medulloblastoma, we used neural-specific inactivation of conditional mutants for DNA DSB repair with associated p53 inactivation. Remarkably, we found that *Ptch1* was specifically lost in all DNA repair-deficient medulloblastomas, and this involvement was also associated with limited other cytogenetic rearrangements that also underpinned these tumors. Therefore, Ptch1 tumor suppressor activity is uniquely required to prevent transformation in cerebellar granule neurons.

Results

Medulloblastoma in DSBR-Deficient Mice. Although germ-line inactivation of *Lig4*, *Xrcc4*, or *Xrcc2* is lethal at mid or early gestation, coincident inactivation of *p53* rescues lethality and promotes a spectrum of tumors by 10 weeks of age, including lymphoma and medulloblastoma (4, 9, 31, 32). To carefully evaluate medulloblastoma exclusive of lymphoma, we generated mice carrying conditional *Lig4* and *Xrcc2* alleles, which were inactivated in neural progenitor cells during development using *Nestin*-cre. Additionally, we also included a Brca2 conditional

Author contributions: P.-O.F., Y.L., H.R.R., and P.J.M. designed research; P.-O.F., Y.L., H.R.R., N.C., K.E.O., and J.Z. performed research; Y.L., N.C., Y.-D.W., K.E.O., N.K., and S.J.B. contributed new reagents/analytic tools; P.-O.F., Y.L., H.R.R., N.C., Y.-D.W., N.K., S.J.B., and P.J.M. analyzed data; and P.-O.F., Y.L., S.J.B., and P.J.M. wrote the paper.

The authors declare no conflict of interest.

This article is a PNAS Direct Submission.

[1]P.-O.F. and Y.L. contributed equally to this work.

[2]To whom correspondence should be addressed. E-mail: peter.mckinnon@stjude.org.

This article contains supporting information online at www.pnas.org/cgi/content/full/0806882106/DCSupplemental.

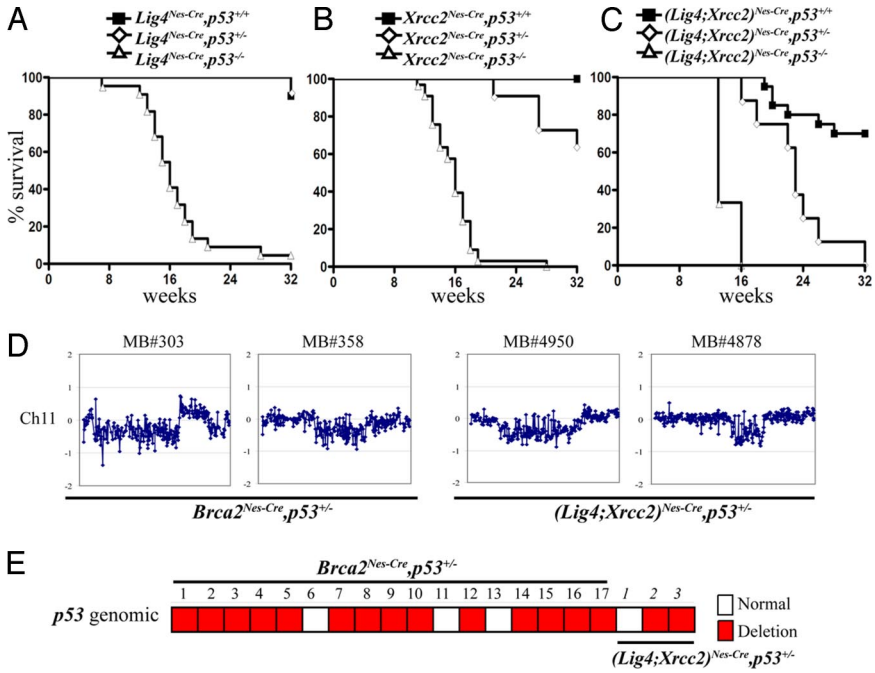

Fig. 1. *p53* deficiency induces medulloblastoma formation in *Lig4*$^{Nes\text{-}Cre}$ and *Xrcc2*$^{Nes\text{-}Cre}$ mice. (*A*) Survival curves of *Lig4*/*p53*-deficient mice. *Lig4*$^{Nes\text{-}Cre}$ ($n = 42$), *Lig4*$^{Nes\text{-}Cre}$, *p53*$^{+/-}$ ($n = 19$), and *Lig4*$^{Nes\text{-}Cre}$; *p53*$^{-/-}$ ($n = 23$) mice were monitored over a period of 32 weeks for survival and medulloblastoma development. The lifespan of *Lig4*$^{Nes\text{-}Cre}$;*p53*$^{-/-}$ mice was significantly shorter compared with the *Lig4*$^{Nes\text{-}Cre}$ and *Lig4*$^{Nes\text{-}Cre}$; *p53*$^{+/-}$ cohort ($P < 0.0001$). (*B*) Survival curves of *Xrcc2*/*p53*-deficient mice. *Xrcc2*$^{Nes\text{-}Cre}$ ($n = 23$), *Xrcc2*$^{Nes\text{-}Cre}$, *p53*$^{+/-}$ ($n = 11$), and *Xrcc2*$^{Nes\text{-}Cre}$, *p53*$^{-/-}$ ($n = 33$) are shown. The lifespan of *Xrcc2*$^{Nes\text{-}Cre}$, *p53*$^{-/-}$ mice was significantly shorter compared with the *Xrcc2*$^{Nes\text{-}Cre}$, *p53*$^{+/-}$ and *Xrcc2*$^{Nes\text{-}Cre}$ ($P < 0.0001$). (*C*) Survival curves of *Ligase4*/*Xrcc2*/*p53*-deficient mice. *Lig4*,*Xrcc2*$^{Nes\text{-}Cre}$ ($n = 20$), *Lig4*,*Xrcc2*$^{Nes\text{-}Cre}$, p53$^{+/-}$ ($n = 8$), *Lig4*,*Xrcc2*$^{Nes\text{-}Cre}$, p53$^{-/-}$ ($n = 3$). The survival curves are statistically significantly different ($P < 0.0001$). (*D*) Representative aCGH analysis of chr11 of *Brca2* and *Lig4*,*Xrcc2*-deficient medulloblastoma associated with *p53* heterozygosity. (*E*) Summary of aCGH results detecting hemizygous deletions of chr11 in medulloblastomas of *Brca2*$^{Nes\text{-}Cre}$ and *Lig4*/*Xrcc2*$^{Nes\text{-}Cre}$. Each column represents a single tumor. Red indicates that the chromosome exhibited genomic loss; regional genomic changes were determined by using a normalized $\log_2$ ratio of ± 0.2 as a cutoff.

knockout as described previously (28) in our study. *Xrcc2*, *Brca2*, and *Lig4* mutants were used to compare the effects of disruption of the 2 mammalian DNA DSB repair pathways, NHEJ (*Lig4*) or HR (*Brca2* and *Xrcc2*). Conditional deletion throughout the nervous system was compatible with animal survival. For simplicity, we refer to *Lig4*$^{LoxP/LoxP}$;*Nestin-cre* mice as *Lig4*$^{Nes\text{-}Cre}$ and have used a similar nomenclature for *Xrcc2* and *Brca2* animals. A notable feature of the conditional mutant animals was the lack of pronounced apoptosis typical after germ-line inactivation of these genes (33, 34), and this likely reflects developmental timing of cre expression (data not shown). However, deletion of Lig4 using Meox2-cre, which expresses in the epiblast cells, leads to a similar neuraxis-wide apoptosis as germ-line Lig4 deletion (data not shown). Nestin-cre-mediated deletion of the Lig4-binding protein Xrcc4 also showed a lack of the neural apoptosis observed when this gene is deleted in the germ line (27).

We initially monitored tumor formation in *Lig4*$^{Nes\text{-}Cre}$, *Xrcc2*$^{Nes\text{-}Cre}$, and *Lig4*/*Xrcc2*$^{Nes\text{-}Cre}$ mice over a period of 32 weeks (Fig. 1 *A–C*). We found that *Lig4*$^{Nes\text{-}Cre}$, *Xrcc2*$^{Nes\text{-}Cre}$, and *Lig4*/*Xrcc2*$^{Nes\text{-}Cre}$ mice developed medulloblastomas between 14 and 16 weeks of age when *p53* was also inactivated [Fig. 1 *A–C* and supporting information (SI) Table S1]. Additionally, *p53* heterozygosity promoted medulloblastomas in (*Lig4*;*Xrcc2*)$^{Nes\text{-}Cre}$ mice, but not in either DNA repair mutant alone, with a tumor onset around 22 weeks of age (Fig. 1*C*). We determined p53 status in medulloblastoma from the (Lig4;Xrcc2)$^{Nes\text{-}Cre}$;*p53*$^{+/-}$ mice by using array comparative genomic hybridization (aCGH) and real-time PCR analysis. We found that the wild-type (WT) *p53* allele was lost (Fig. 1 *D* and *E*), implying that *p53* loss of heterozygosity (LOH) contributed to medulloblastoma, probably reflecting increased genomic instability when both repair pathways are inactivated. For comparison to the *Lig4* and *Xrcc2*-deficient mice, we also evaluated chromosome 11 loss in *Brca2*$^{Nes\text{-}Cre}$;*p53*$^{+/-}$ tumors and also observed inactivation of the remaining WT *p53* allele in most cases (Fig. 1 *D* and *E*).

Defective DNA DSB Repair Leads to Specific Inactivation of Ptch1. Multiple medulloblastomas from the different repair mutants were analyzed by using aCGH and spectral karyotyping (SKY). We detected chromosome 13 alterations as a common event in medulloblastoma, which involved loss or translocation of 1 copy of chromosome 13 (Fig. 2 *A–C* and Table S2). Analysis of the region of chr13 involved in the translocations by using aCGH revealed that in all cases it involved *Ptch1*, suggesting that *Ptch1* inactivation was a key target in medulloblastoma formation. Because 1 copy of *Ptch1* was inactivated through chromosome loss or translocation, we determined the status of the remaining *Ptch1* allele. To do this, we sequenced *Ptch1* mRNA via cDNA amplification and found mutations in the remaining *Ptch1* allele in all tumors analyzed ($n = 20$; Fig. 2*D* and Table S3). In most cases, these mutations led to a truncated Ptch1 protein that would be predicted to inactivate Ptch1 or substantially affect function. To confirm that these were bona fide tumor-related *Ptch1* mutations that arose from genomic mutation, we sequenced the corresponding regions of genomic DNA. We found that in all cases, genomic DNA from the tumors contained the corresponding mutation found in the cDNA. These included splice donor–acceptor mutations that would predict exon skipping, as observed in the tumor-derived *Ptch1* cDNA. We also confirmed that inactivation of *Ptch1* was central to tumor formation by evaluating the tumor latency and *Ptch1* status in *Ptch1*$^{+/-}$ compound mutants. We generated *Brca2*$^{Nes\text{-}Cre}$;*Ptch1*$^{+/-}$;*p53*$^{+/-}$ (or *p53*$^{-/-}$) mice and compared tumor latency between various related genotypes (Fig. S1). Latency was dramatically reduced (<5 weeks) in *Brca2*$^{Nes\text{-}Cre}$;*Ptch1*$^{+/-}$;*p53*$^{-/-}$ mice, and aCGH or PCR analysis of

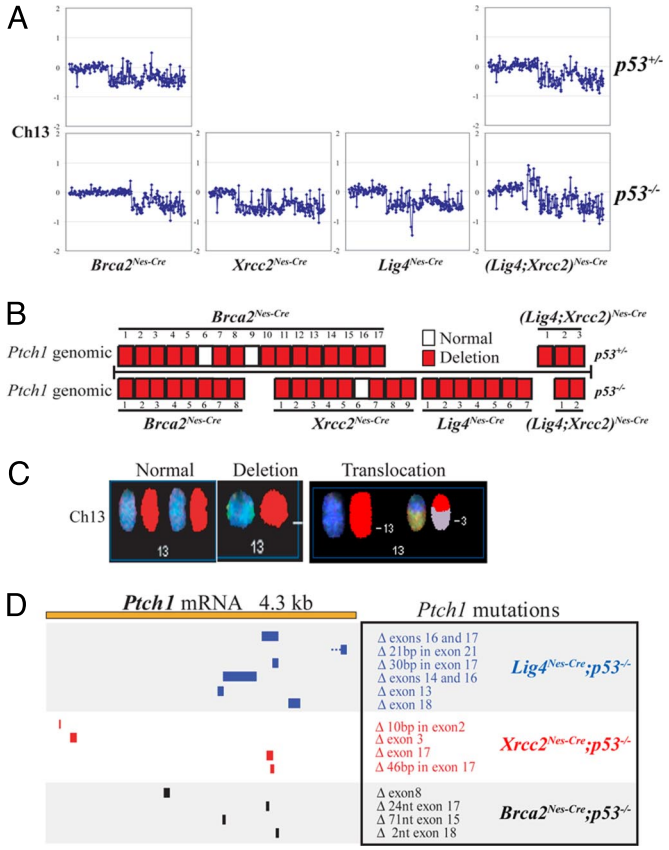

Fig. 2. *Ptch1* is lost in DSBR-deficient medulloblastomas. (*A*) Representative aCGH analysis of chr13 of *Brca2*, *Lig4*, *Xrcc2*-deficient medulloblastomas in *p53* mutant backgrounds. (*B*) Summary of aCGH results detecting deletions of chr13 in the medulloblastomas. Each column represents a single tumor, and each line represents 1 chromosome. Each red square indicates that the chromosome exhibited genomic loss. (*C*) Representative FISH analysis of chr13 showing either deletion or translocation. (*D*) Sequence analysis of *Ptch1* mRNA from *Lig4*, *Xrcc2*, and *Brca2*-deficient medulloblastoma.

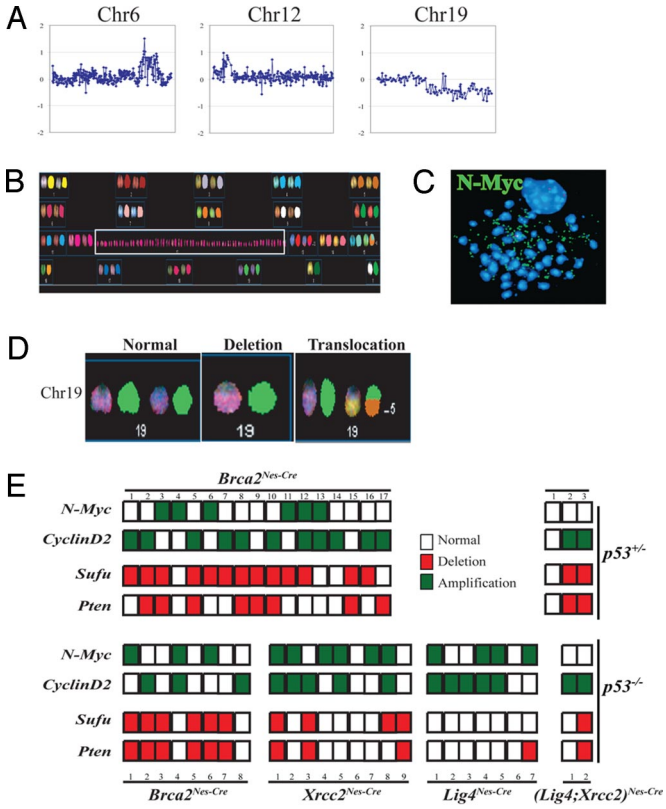

Fig. 3. Genomic analysis of chromosomes 6, 12, and 19 in medulloblastomas. (*A*) Representative aCGH of chromosomes 6, 12, and 19 in medulloblastomas examined. (*B*) Representative complete SKY analysis of *Brca2*$^{Nes\text{-}Cre}$, *p53*$^{-/-}$ showing a large number of double minutes, indicated by a white box. (*C*) FISH analysis for *N-Myc* amplification in medulloblastoma (Magnification: 1,000×). (*D*) Representative SKY of chr19 showing either deletion or translocation. (*E*) Summary of the genomic rearrangements of *N-Myc*, *cylin D2*, *Sufu*, and *Pten* in the medulloblastomas. Each column represents a single tumor, and each line represents 1 chromosome. Each red square indicates that the chromosome exhibited genomic loss, whereas each green square indicates a region of genomic amplification.

the resulting tumors showed loss of the remaining WT *Ptch1* allele (and also *p53* in the case of *Brca2*$^{Nes\text{-}Cre}$;*Ptch1*$^{+/-}$;*p53*$^{+/-}$) (Fig. S1 *B* and *C*). These data indicate that loss of *Ptch1* is closely linked to the genesis of medulloblastoma.

Up-Regulation of the Shh Pathway in Medulloblastoma. Ptch1 functions to modulate Smoothened activation of Gli1 transcriptional activity (35). Consistent with a loss of Ptch1 function, activation of the Shh pathway was found in all medulloblastomas analyzed (n = 16; Fig. S2*A*). A similar gene expression profile occurred in all medulloblastomas with up-regulation of a common cohort of genes, including known target genes of the Shh-signaling pathway, such as *Math1*, *sFrp1*, *Ptch2*, *Gli1*, *N-Myc*, *Sox18*, and *D-Cyclins*. Other genes not (yet) directly linked to Shh signaling also were strongly up-regulated by array analysis in the tumors, such as Titest, a gene of unknown function. We confirmed the microarray expression profiles by using real-time PCR to compare with wild-type or *p53*$^{-/-}$ P5 and adult cerebella (Fig. S2*B*). Together, these data indicate that tumorigenesis associated with disruption of DSB repair results in *Ptch1* inactivation and up-regulation of the Shh pathway.

N-Myc or Cyclin D2 Is Amplified in the DSB Repair-Deficient Medulloblastomas. Although loss of *Ptch1* was a defining event in all medulloblastomas, other recurring chromosomal changes were also present. These included amplification of regions of chr12 and chr6, corresponding to *N-Myc* and *cyclin D2* and, more selectively, loss of a portion of chr19 in medulloblastoma associated with tumors arising in *Brca2* mutants or after coinactivation of *Lig4* and *Xrcc2* (Fig. 3). We found that the *N-Myc* locus was amplified on chr12 in medulloblastoma samples spanning all DNA repair mutant genotypes (Fig. 3 A and *E*). In some cases, *N-Myc* amplification was reflected by abundant double-minute chromosomes; we confirmed *N-Myc* amplification in those tumors using FISH and found a strong signal corresponding to multiple copies of *N-Myc* (Fig. 3*C*).

Although *N-Myc* amplification was a prominent feature in medulloblastomas, tumors not showing genomic *N-Myc* alterations were often associated with an amplification of chr6, suggesting a reciprocal relationship between N-Myc and Cyclin D2 amplification. Because cyclin D2 is expressed at high levels in medulloblastoma and is located on chr6, we confirmed the involvement of cyclin D2 in many of the *Brca2*$^{Nes\text{-}Cre}$;*p53*$^{-/-}$ tumors by using aCGH to map the region of chr6 that was amplified (Fig. 3 *A* and *E*) and cyclin D2 FISH (data not shown). The chromosomal changes associated with these events probably augment initial mutations acquired by the tumor; however, because these genes are also Shh targets, this probably also contributes to enhanced expression of N-Myc and cyclin D2 in the tumors. Thus, *Ptch1* loss and subsequent up-regulation of SHH signaling also will promote increased N-Myc and cyclin D2

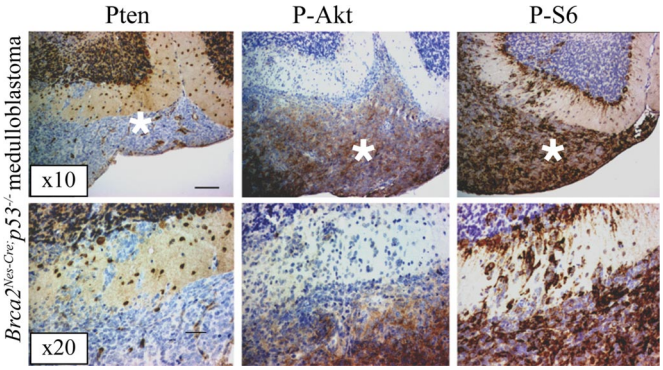

Fig. 4. Pten pathway disruption in Brca2-deficient medulloblastoma. Shown are representative medulloblastoma sections showing loss of expression of Pten and up-regulation of levels of phospho-Ser-473 of Akt (*p*-Akt) and phospho-serine 235 and 236 of S6 (*p*-S6) in $Brca2^{Nes\text{-}cre};p53^{-/-}$-deficient medulloblastoma. Asterisks denote tumor tissue. (Scale bar: *Upper*, 0.1 mm; *Lower*, 0.05 mm.)

expression. Either *N-Myc* or *cyclin D2* amplification during tumor progression would contribute to the evolution of medulloblastoma by providing a potent growth advantage.

Defective Homologous Recombination Targets Chromosome 19. A loss or translocation of chr19 was associated with tumors in which HR was disabled (Fig. 3*D* and Table S2). By using aCGH, we found that *Brca2*-deficient (19/25), *Xrcc2*-deficient (3/9), and *Ligase4*/*Xrcc2*-deficient tumors (4/5), but not *Lig4*-deficient tumors, were associated with chr19 alterations, a finding consistent with the presence of a tumor suppressor gene on this chromosome. The sporadic loss of chr19 has also been reported in some other mouse medulloblastoma models (12, 36). The commonly lost region of chromosome 19 in our study is syntenic with human chromosome 10q, which is frequently lost in medulloblastoma (37–39). Known tumor suppressors in this region include *PTEN* and *SUFU*. Although frequent gene-specific mutations of *PTEN* have not been reported in medulloblastoma, gross alterations of *PTEN* are commonly found in BRCA1-defective breast cancers, showing that *PTEN* was selectively targeted in a setting of defective HR repair (40). *SUFU* loss also has been directly linked to medulloblastoma (25, 41). Therefore, we examined these 2 tumor suppressors for evidence of biallelic inactivation in our medulloblastoma models.

Both *Sufu* and *Pten* were coordinately deleted at very high frequencies (Fig. 3*E*). Sequence analysis of *Sufu* cDNA derived from tumors ($n = 5$) did not reveal mutations, and *Sufu* expression was detected in all tumors, suggesting that a gene(s) other than *Sufu* was the important target on chr19. Next, we determined whether Pten was selectively inactivated in HR-deficient tumors, but we did not find any mutations in the complete ORF of *Pten* cDNA from tumors ($n = 8$; data not shown). However, an immunohistochemical survey of Pten expression in 8 different Brca2-deficient tumor samples with chr19 deletion showed that all tumors had partial or complete loss of Pten immunoreactivity accompanied by variable levels of increased phospho-Akt (Ser-473) and phospho-S6 (Ser 235, 236), consistent with heterogeneous inactivation of Pten and increased signaling through downstream effectors in the PI3K signaling pathway (Fig. 4). Pten expression was variably altered, with 2 tumors showing complete loss of expression throughout the tumor, whereas the remaining tumors showed regions lacking Pten expression intermixed with regions that retained Pten expression predominantly in the cytoplasm, and normal granule neurons showed expression in both the nucleus and cytoplasm. Thus, biallelic mutations of *Pten* were not identified, but Pten inactivation or signaling abnormalities were observed frequently in HR-deficient medulloblastomas.

Discussion

To further characterize the tumor-suppressor role of DNA DSB repair pathways in defined tissues, we used conditional inactivation of *Lig4*, *Xrcc2*, and *Brca2* throughout the nervous system and found that in conjunction with *p53* mutations, rapid development of medulloblastoma occurred. A key finding from our data is the identification of *Ptch1* as a critical target in all DNA repair-deficient medulloblastomas, indicating the essential tumor-suppressor function of this gene for preventing transformation of GNPs.

DNA repair deficiency provides an unbiased means to select for important tumor-promoting mutations, and in this setting we found that *Ptch1* was consistently targeted in medulloblastoma. In Gorlin syndrome, where individuals inherit a germ-line *PTCH1* mutation, cancer occurs in about 5% of cases, and in $Ptch1^{+/-}$ mice it is strain-dependent with an incidence between 5% and 15%. Medulloblastoma in $Ptch1^{+/-}$ mice is associated with *Ptch1* loss in preneoplastic lesions found as incipient medulloblastoma in which the Shh pathway is up-regulated (21, 42). Active Shh signaling is a potent growth-promoting activity, and it will contribute significantly to growth and expansion of GNP cells (7). Although PTCH1 loss is strongly linked to medulloblastoma, disruption of the Shh pathway accounts for only a fraction (≈30%) of medulloblastomas (6, 7).

Although it is possible that the *Ptch1* locus is particularly susceptible to DNA damage, it seems more likely that loss of DNA repair capacity will randomly and effectively select for the mutation conferring the most potent cellular growth advantage. Given the high incidence of tumors associated with Ptch1 haploinsufficieny, it is likely that inactivation of 1 copy of Ptch1 (via translocation or chromosome loss) will drive selection for inactivation of the second allele. Perhaps initial loss of a copy of *Ptch1* promotes enhanced proliferation via mild mitigation of Smoothened inhibition of Shh signaling, leading to an increase in replication stresses, such as premature termination, replication fork collapse, and generation of DNA DSBs (43). Alternatively, random mutation acquisition in the abundant granule cell population may serve as a reservoir of cooperating mutations, among which bi-allelic Ptch1 loss will occur.

Together with *Ptch1* inactivation, we also observed *N-Myc* or *CyclinD2* amplification in medulloblastomas. Both of these are Gli targets; N-Myc is critical for GNP proliferation (44–46), whereas the D-cyclins influence cerebellar development and GNP proliferation (47–50). Thus, loss of Ptch1 function will lead to a Gli-dependent transcriptional up-regulation of N-Myc and cyclin D2. In addition to increased expression of N-Myc as a result of Ptch1 loss and activated Shh signaling, we also found genomic amplification of *N-Myc* and *CyclinD2* in the medulloblastomas, suggesting that there is a significant advantage to a tumor cell for additional up-regulation of the growth-promoting factors beyond that induced by increased Shh signaling. Consistent with our data, N-Myc amplification also has been found in medulloblastomas arising after inactivation of *Xrcc4* (27). There also appeared to be a reciprocal relationship between N-Myc and Cyclin D2 genomic amplification, suggesting that amplification of only one of these oncogenes was required for medulloblastoma development. The tumorigenic properties of Myc have been linked recently to a function during DNA replication via interactions with minichromosome maintenance subunits to participate in the control of DNA replication origin activity (51). Therefore, increased expression of N-Myc may lead to increased replication firing and associated DNA damage and checkpoint activation (51), generating a compounding scenario in DNAR-deficient GNPs that significantly promotes oncogenic mutation accumulation.

Finally, we observed genomic rearrangements and losses of chr19 in medulloblastoma arising in the context of defective HR, but not in tumors associated with defective NHEJ. Importantly, human medulloblastomas show frequent allelic losses of human chromosome 10q, syntenic to the commonly lost region of mouse chr19. In both human medulloblastoma and mouse tumors studied here, the most commonly deleted region includes the well-described tumor suppressors *SUFU* and *PTEN*, with a minor percentage of tumors that retain both copies of *PTEN* but delete *SUFU* (39). Inherited mutations in *SUFU*, a negative regulator of SHH signaling, cause inherited predisposition to medulloblastoma; however, somatic biallelic inactivation of *SUFU* occurs in less than 1% of sporadic medulloblastoma (39, 41, 52, 53). Similarly, biallelic inactivation of *PTEN* occurs infrequently in medulloblastoma (54). We did not identify any mutations in the remaining allele of *Pten* or *Sufu* from tumors with chr19 loss. Thus, medulloblastoma arising in the context of HR deficiency in the mouse showed selective recurrent chromosomal imbalances that were highly similar to those mapped in human medulloblastoma and do not appear to target *Sufu* or *Pten* for biallelic inactivation.

Despite the lack of mutations inducing complete loss of PTEN function, reduced expression of PTEN and evidence of elevated AKT signaling were shown in human medulloblastoma (54). We also found evidence of loss of Pten expression and concomitant increase in phospho-Akt (Ser-473) in all Brca2-deficient tumors evaluated. The extent of Pten loss was variable, with some tumors showing a uniform absence of Pten and others displaying clusters of Pten-deficient tumor cells intermixed with Pten-positive adjacent tumor cells. Although we did not identify intragenic inactivating mutations in *Pten*, haploinsufficiency of *Pten* may strongly promote tumorigenesis, as has been shown in mouse prostate, and modifiers of Pten stability may also decrease levels of Pten protein (55, 56). Engineered loss of Pten or expression of a constitutively active Akt can synergize with engineered dysregulation of SHH signaling in mouse models to generate medulloblastoma (57). Both pathways were targeted by somatic changes arising in medulloblastoma with defective HR, which showed abnormalities in Pten and PI3K signaling in combination with biallelic inactivation of *Ptch1*.

It is likely that defective DNA repair generates a continuum of genomic alterations during cell proliferation that allow for uncoupling of the growth controls of the GNPs. The genomic changes we identified in this study reflect the specific minimal changes that are required to transform granule neurons in vivo, providing the blueprint for GNP transformation. The models described here will be important for further deciphering tissue-specific disruption of genomic stability and tumorigenesis.

Materials and Methods

Generation of *Brca2*$^{Nes\text{-}Cre}$, *Xrcc2*$^{Nes\text{-}Cre}$, *Ligase4*$^{Nes\text{-}Cre}$, *p53*-Deficient Mice. *Brca2*$^{Nes\text{-}Cre}$ and *Xrcc2*$^{Nes\text{-}Cre}$ were generated as described previously (4, 26, 28) and crossed with *p53*$^{+/-}$ mice to obtain the various groups used in this study. The conditional Lig4 mouse contains LoxP sites surrounding the single *Lig4* coding exon and was generated by standard methods. Tumor formation was monitored over a period of 8 months.

Genomic Analysis. Genomic DNA was prepared from brain tumors by using the DNeasy blood and tissue kit (Qiagen), and metaphase spreads were from tumors after injection of colcemid (28). SKY and aCGH analysis were performed as described previously (20, 25). Copy number changes of gene regions in aCGH were determined by using a normalized $\log_2$ ratio of ± 0.2 as a cutoff. Primers used for isolation and analyses of *Ptch1* and *Sufu* are listed in *SI Text*.

Immunohistochemistry. Immunohistochemistry was conducted by using antigen retrieval with the following antibodies: Pten (1:100; 9559; Cell Signaling Technology), *p*-Akt (Ser-473) (1:50; 9271; Cell Signaling Technology), and *p*-S6 (Ser-235/236) (1:500; 2211; Cell Signaling Technology). Immunodetection was with biotinylated secondary antibodies followed by peroxidase-avidin and DAB substrate (Elite ABC; Vector Laboratories).

ACKNOWLEDGMENTS. We thank the Hartwell Center, the Cancer Center Cytogenetics Core, and the Transgenic Core facility at St. Jude Children's Research Hospital for their support of this work. These studies were supported by National Institutes of Health Grants CA-21765 and CA096832, Cancer Center Support Grant P30 CA21765, a fellowship from the Canadian Institutes of Health Research (to N.C.), and the American Lebanese and Syrian Associated Charities (ALSAC) of St. Jude Children's Research Hospital.

1. West SC (2003) Molecular views of recombination proteins and their control. *Nat Rev Mol Cell Biol* 4:435–445.
2. Wyman C, Kanaar R (2006) DNA double-strand break repair: All's well that ends well. *Annu Rev Genet* 40:363–383.
3. Bassing CH, Alt FW (2004) The cellular response to general and programmed DNA double strand breaks. *DNA Repair (Amst)* 3:781–796.
4. Orii KE, Lee Y, Kondo N, McKinnon PJ (2006) Selective utilization of nonhomologous end-joining and homologous recombination DNA repair pathways during nervous system development. *Proc Natl Acad Sci USA* 103:10017–10022.
5. Lee Y, McKinnon PJ (2007) Responding to DNA double strand breaks in the nervous system. *Neuroscience* 145:1365–1374.
6. Gilbertson RJ, Ellison DW (2008) The origins of medulloblastoma subtypes. *Annu Rev Pathol* 3:341–365.
7. Wechsler-Reya R, Scott MP (2001) The developmental biology of brain tumors. *Annu Rev Neurosci* 24:385–428.
8. Kho AT, *et al.* (2004) Conserved mechanisms across development and tumorigenesis revealed by a mouse development perspective of human cancers. *Genes Dev* 18:629–640.
9. Lee Y, *et al.* (2003) A molecular fingerprint for medulloblastoma. *Cancer Res* 63:5428–5437.
10. Tong WM, *et al.* (2003) Null mutation of DNA strand break-binding molecule poly(ADP-ribose) polymerase causes medulloblastomas in p53(−/−) mice. *Am J Pathol* 162:343–352.
11. Uziel T, *et al.* (2005) The tumor suppressors Ink4c and p53 collaborate independently with Patched to suppress medulloblastoma formation. *Genes Dev* 19:2656–2667.
12. Zindy F, *et al.* (2007) Genetic alterations in mouse medulloblastomas and generation of tumors de novo from primary cerebellar granule neuron precursors. *Cancer Res* 67:2676–2684.
13. Bakhshi S, *et al.* (2003) Medulloblastoma with adverse reaction to radiation therapy in nijmegen breakage syndrome. *J Pediatr Hematol Oncol* 25:248–251.
14. Huang J, *et al.* (2008) Mutations in the nijmegen breakage syndrome gene in medulloblastomas. *Clin Cancer Res* 14:4053–4058.
15. Offit K, *et al.* (2003) Shared genetic susceptibility to breast cancer, brain tumors, and Fanconi anemia. *J Natl Cancer Inst* 95:1548–1551.
16. Dellovade T, Romer JT, Curran T, Rubin LL (2006) The hedgehog pathway and neurological disorders. *Annu Rev Neurosci* 29:539–563.
17. Giordana MT, *et al.* (2002) MDM2 overexpression is associated with short survival in adults with medulloblastoma. *Neuro Oncol* 4:115–122.
18. Woodburn RT, Azzarelli B, Montebello JF, Goss IE (2001) Intense p53 staining is a valuable prognostic indicator for poor prognosis in medulloblastoma/central nervous system primitive neuroectodermal tumors. *J Neurooncol* 52:57–62.
19. Goodrich LV, Milenkovic L, Higgins KM, Scott MP (1997) Altered neural cell fates and medulloblastoma in mouse patched mutants. *Science* 277:1109–1113.
20. Lee Y, *et al.* (2006) Patched2 modulates tumorigenesis in patched1 heterozygous mice. *Cancer Res* 66:6964–6971.
21. Oliver TG, *et al.* (2005) Loss of patched and disruption of granule cell development in a pre-neoplastic stage of medulloblastoma. *Development* 132:2425–2439.
22. Wetmore C, Eberhart DE, Curran T (2001) Loss of p53 but not ARF accelerates medulloblastoma in mice heterozygous for patched. *Cancer Res* 61:513–516.
23. Jacks T, *et al.* (1994) Tumor spectrum analysis in p53-mutant mice. *Curr Biol* 4:1–7.
24. Marino S (2005) Medulloblastoma: Developmental mechanisms out of control. *Trends Mol Med* 11:17–22.
25. Lee Y, *et al.* (2007) Loss of suppressor-of-fused function promotes tumorigenesis. *Oncogene* 26:6442–6447.
26. Lee Y, McKinnon PJ (2002) DNA ligase IV suppresses medulloblastoma formation. *Cancer Res* 62:6395–6399.
27. Yan CT, *et al.* (2006) XRCC4 suppresses medulloblastomas with recurrent translocations in p53-deficient mice. *Proc Natl Acad Sci USA* 103:7378–7383.
28. Frappart PO, Lee Y, Lamont J, McKinnon PJ (2007) BRCA2 is required for neurogenesis and suppression of medulloblastoma. *EMBO J* 26:2732–2742.
29. Holcomb VB, Vogel H, Marple T, Kornegay RW, Hasty P (2006) Ku80 and p53 suppress medulloblastoma that arise independent of Rag-1-induced DSBs. *Oncogene* 25:7159–7165.
30. Pazzaglia S, *et al.* (2002) High incidence of medulloblastoma following X-ray-irradiation of newborn Ptc1 heterozygous mice. *Oncogene* 21:7580–7584.
31. Frank KM, *et al.* (2000) DNA ligase IV deficiency in mice leads to defective neurogenesis and embryonic lethality via the p53 pathway. *Mol Cell* 5:993–1002.
32. Gao Y, *et al.* (2000) Interplay of p53 and DNA-repair protein XRCC4 in tumorigenesis, genomic stability and development. *Nature* 404:897–900.
33. Barnes DE, Stamp G, Rosewell I, Denzel A, Lindahl T (1998) Targeted disruption of the gene encoding DNA ligase IV leads to lethality in embryonic mice. *Curr Biol* 8:1395–1398.

34. Gao Y, *et al.* (1998) A critical role for DNA end-joining proteins in both lymphogenesis and neurogenesis. *Cell* 95:891–902.
35. Lum L, Beachy PA (2004) The Hedgehog response network: Sensors, switches, and routers. *Science* 304:1755–1759.
36. Shakhova O, Leung C, van Montfort E, Berns A, Marino S (2006) Lack of Rb and p53 delays cerebellar development and predisposes to large cell anaplastic medulloblastoma through amplification of N-Myc and Ptch2. *Cancer Res* 66:5190–5200.
37. Lo KC, Rossi MR, Eberhart CG, Cowell JK (2007) Genome wide copy number abnormalities in pediatric medulloblastomas as assessed by array comparative genome hybridization. *Brain Pathol* 17:282–296.
38. Russo C, *et al.* (1999) Comparative genomic hybridization in patients with supratentorial and infratentorial primitive neuroectodermal tumors. *Cancer* 86:331–339.
39. Scott DK, *et al.* (2006) Identification and analysis of tumor suppressor loci at chromosome 10q23.3–10q25.3 in medulloblastoma. *Cell Cycle* 5:2381–2389.
40. Saal LH, *et al.* (2008) Recurrent gross mutations of the PTEN tumor suppressor gene in breast cancers with deficient DSB repair. *Nat Genet* 40:102–107.
41. Taylor MD, *et al.* (2002) Mutations in SUFU predispose to medulloblastoma. *Nat Genet* 31:306–310.
42. Yang ZJ, *et al.* (2008) Medulloblastoma can be initiated by deletion of Patched in lineage-restricted progenitors or stem cells. *Cancer Cell* 14:135–145.
43. Branzei D, Foiani M (2005) The DNA damage response during DNA replication. *Curr Opin Cell Biol* 17:568–575.
44. Hatton BA, *et al.* (2006) N-myc is an essential downstream effector of Shh signaling during both normal and neoplastic cerebellar growth. *Cancer Res* 66:8655–8661.
45. Kenney AM, Cole MD, Rowitch DH (2003) Nmyc upregulation by sonic hedgehog signaling promotes proliferation in developing cerebellar granule neuron precursors. *Development* 130:15–28.
46. Oliver TG, *et al.* (2003) Transcriptional profiling of the Sonic hedgehog response: A critical role for N-myc in proliferation of neuronal precursors. *Proc Natl Acad Sci USA* 100:7331–7336.
47. Ciemerych MA, *et al.* (2002) Development of mice expressing a single D-type cyclin. *Genes Dev* 16:3277–3289.
48. Huard JM, Forster CC, Carter ML, Sicinski P, Ross ME (1999) Cerebellar histogenesis is disturbed in mice lacking cyclin D2. *Development* 126:1927–1935.
49. Pogoriler J, Millen K, Utset M, Du W (2006) Loss of cyclin D1 impairs cerebellar development and suppresses medulloblastoma formation. *Development* 133:3929–3937.
50. Zindy F, *et al.* (2006) N-Myc and the cyclin-dependent kinase inhibitors p18Ink4c and p27Kip1 coordinately regulate cerebellar development. *Proc Natl Acad Sci USA* 103:11579–11583.
51. Dominguez-Sola D, *et al.* (2007) Non-transcriptional control of DNA replication by c-Myc. *Nature* 448:445–451.
52. Koch A, *et al.* (2004) No evidence for mutations or altered expression of the Suppressor of Fused gene (SUFU) in primitive neuroectodermal tumours. *Neuropathol Appl Neurobiol* 30:532–539.
53. Thompson MC, *et al.* (2006) Genomics identifies medulloblastoma subgroups that are enriched for specific genetic alterations. *J Clin Oncol* 24:1924–1931.
54. Hartmann W, *et al.* (2006) Phosphatidylinositol 3′-kinase/AKT signaling is activated in medulloblastoma cell proliferation and is associated with reduced expression of PTEN. *Clin Cancer Res* 12:3019–3027.
55. Wang X, *et al.* (2007) NEDD4–1 is a proto-oncogenic ubiquitin ligase for PTEN. *Cell* 128:129–139.
56. Trotman LC, *et al.* (2003) Pten dose dictates cancer progression in the prostate. *PLoS Biol* 1:E59.
57. Hambardzumyan D, *et al.* (2008) PI3K pathway regulates survival of cancer stem cells residing in the perivascular niche following radiation in medulloblastoma in vivo. *Genes Dev* 22:436–448.